The postnatal development of large light and small dark neurons in mouse dorsal root ganglia: a statistical analysis of cell numbers and size

S. N. LAWSON

Department of Physiology, The Medical School, University Walk, Bristol BS8 1TD, England

Summary

A method is described for the analysis of cell types in mouse dorsal root ganglia using the distribution of cell cross-sectional areas measured at the level of the nucleolus in 1.5 μm Epon sections. Using a computer program it was possible to demonstrate the existence of two normally distributed sub-populations of neurons in all the 3rd lumbar segment ganglia (17 in number) measured at various ages from birth to 70 days. The two populations appeared to correspond with large light cells and small dark cells. The large light cell bodies increased in size until about 20 days postnatal, subsequently their size decreased whereas the mean size of the small dark cells reached a plateau by about day 10. The relationship of both nuclear volume and surface area to the surface area of the perikaryon differed between light and dark cells. The number of neurons in L_3 remained virtually constant at about 6000 throughout the period examined. Since the proportion of neurons in each population was not shown to change with age there was no evidence that cells could change from one type into the other.

Introduction

It is generally held that neurons in the dorsal root ganglion (DRG) fall into at least two categories on the basis of their size, appearance and histochemical reactions (Hatai, 1902; Preto Parvis, 1954; Andres, 1961; Kalina and Wolman, 1970; Parfianowicz *et al.*, 1971; Yamadori, 1971; Lawson *et al.*, 1974; Boutry and Novikoff, 1975). The two main categories have been called A and B cells by Andres (1961) and large light and small dark cells by others (for a review of the literature see Lieberman, 1976). Under the light microscope, the large light cells generally have a much lighter more coarsely granular or clumped-looking cytoplasm, whereas the smaller cells tend to have a darker, apparently denser, more uniform cytoplasm. This appearance can be explained on ultrastructural examination: the larger neurons are paler staining (less osmiophilic) with clumped groupings of endoplasmic reticulum (ER) and ribosomes and a sparse distribution of organelles between which are less electron-dense areas containing many neurofilaments. The small cells are darker with more compactly and evenly distributed rough ER and other organelles but with

apparently fewer filamentous structures (Lieberman, 1976). Other differences between the above cell types have included greater concentrations of acid phosphatase (Sarrat, 1970), acid β-glycerophosphatase, acetylcholinesterase, and monoamine oxidase (Kalina and Wolman, 1970), in the small cells than in the larger ones.

Some of the basic differences between these two cell types could result from a greater packing density of organelles in the small cells, resulting in apparently greater concentrations and indeed there has been little attempt to show quantitatively that large light cells and small dark cells are from separate populations and are not merely examples of the extreme ends of a single distribution. The first clear evidence of a discontinuous distribution implying more than one distinct cell category was provided by Hughes (1973) who used the probability paper method described by Harding (1949) to demonstrate the existence of two normally distributed populations in opossum DRGs on the basis of cell diameter. Frequency distributions of neuronal diameters in adult human sacral DRGs also showed a peak at the smaller sizes with a superimposed hump at larger diameters (Ohta *et al.*, 1974). However, more recently it has been suggested that three cell types can be distinguished in human L_5 DRGs by the appearance of frequency distributions of cell diameters. (Kawamura and Dyck, 1978).

In a previous paper (Lawson *et al.*, 1974), a study of cell birthdays was related to cell size measurements. It became apparent during this study that a quantitative approach to the analysis of cell populations within the DRG was essential, (a) if a study of the development of the different cell types was to be undertaken and (b) to obtain the basis for evaluating precise quantitative information on abnormalities in particular cell types in mutants or disease states. The present paper on mouse DRGs describes a method for lending greater precision to the quantitation of cell size than that used to date in this tissue, allied with a statistical method of data analysis enabling the frequency distribution histograms to be analysed into component populations.

Methods

Male 129/ReJ mice were used. The day on which mice were born was designated day 0.

CELL COUNTS

Mice anaesthetized with Nembutal were perfused through the left ventricle with normal saline followed by Bouin's fixative. The ganglia were carefully dissected out and placed in Bouin's. After processing and embedding in paraffin wax, serial 10 μm sections were cut. A 'portwine' haematoxylin and eosin method was used to stain all ganglia as follows. The dewaxed sections were stained for 2 h in Erlich's haematoxylin (80 drops in 100 ml distilled water), rinsed in Scott's tap water (Scott, 1912) for 2 min, rinsed in distilled water and stained in 1% aqueous eosin for 30 s. After rinsing in distilled water they were dehydrated, cleared and mounted. This method stains chromatin blue and nucleoli bright red. Such clear contrast is particularly necessary for identification of nucleoli in newborn mice. Using a x 40 objective all the neurons with nucleoli in every alternate section were counted. The counts from each section were added together, and doubled to find the total number per ganglion. A drawing tube attachment which superimposed a grid on the section helped to avoid any duplication in counting.

Errors

Abercrombie's (1946) correction factor for split nucleoli was not used as it has been shown by Cammermeyer (1967), that nucleoli in formaldehyde fixed sections are very rarely split; more usually they are displaced into one section or the other. There is no reason to believe that Bouin-fixed nucleoli behave differently. Another type of error would result if the proportion of cells with multiple nucleoli changed with age. The percentage of counted neurons with more than one nucleolus apparent are plotted in Fig. 1B. There is no correlation between this percentage and age. Any errors resulting from multiple nucleoli were therefore considered to be constant throughout the ages studied and for comparative purposes could be ignored.

CELL AREA MEASUREMENTS

Mice of 1—2, 10, 20, 34, 50—60 and 74 days were anaesthetized with Nembutal, and fixed by perfusion with 1% glutaraldehyde and 1% paraformaldehyde in 0.12 M phosphate buffer (Palay and Chan-Palay, 1974). The ganglia were dissected out, left in the fixative for 1 h, washed in buffer and postfixed in 2% osmium tetroxide in phosphate buffer for 1 h. They were washed in 0.1 M maleic acid, dehydrated and embedded in Epon. Three consecutive 1.5 μm sections were cut at intervals of 120 μm throughout the ganglion. These were stained with methylene blue and examined under a Reichert Biopan or Biovar microscope with x 100 oil immersion objective. Cell cross-sectional areas were measured (using a drawing tube attachment for the microscope) by drawing the cell outline directly in the field of a Graf pen digitizing tablet. This generated a series of X-Y co-ordinates from which the area circumscribed by the perimeter was calculated by a Tektronix 4051 computer (Biscoe *et al.*, 1978). The computed data was stored on tape for subsequent analyses. The areas were computed directly in $μm^2$ using a magnification factor measured directly at every session with a stage micrometer. Only sections of cells with clear large nucleolar profiles were measured; from experience these were expected to be larger in the larger cells. Cells with very pale staining, or very small nucleolar sections were excluded. The areas of all such cells were measured in one of the 1.5 μm sections at 120 μm intervals throughout the ganglion (approximately 200 cells per ganglion). When sufficient data had been collected, the computer generated frequency distribution histograms of the areas (Biscoe *et al.*, 1978).

ANALYSIS OF FREQUENCY DISTRIBUTION HISTOGRAMS

The cell area frequency distribution histograms (Figs. 2, 3 and 5) obtained as described above were clearly comprised of more than one component distribution. They were therefore analysed to find the number, sizes and shapes of the component distributions. Two methods were used. The first was unsatisfactory and is included only to exemplify the problems encountered; the second, more sophisticated version using a complex computer program is the preferred method.

First method

At least two L_3 ganglia from different mice were analysed at each of the ages. From the frequency distribution histograms obtained, (Fig. 2) estimations were made of the number of populations of neurons, the proportion of cells in each population and the mean and standard deviation of each population using probability paper (Harding 1949; Lawson *et al.*, 1977) or by fitting curves to the histograms by eye. For each combination of such values a simple program calculated the expected overall frequency distribution and the χ^2 statistic for goodness of fit. By trial and error the estimates were adjusted so as to improve the fit (reduce the value of χ^2) of the expected to the observed frequency distribution; if $P > 0.05$, the sum of the proposed populations is not significantly different at the 5% level from the observed histogram and these values therefore gave one possible solution to the histogram. 50—150 different χ^2 tests were necessary for each histogram proposing parameters for 2, 3 and 4 populations of cells.

Second method

The frequency distribution histogram (observed data) was analysed using the 'Maximum Likelihood Program' (MLP) written by G. J. S. Ross from the Statistics Department of Rothamsted Experimental Station, Harpenden, Herts. This program became available after the above analysis was completed. The program used the method of maximum likelihood to estimate the parameters of each distribution selected by the user (for example, one normal distribution, a mixture of two normal distributions, log normal distribution, etc.). That is, the parameter estimates (mean, proportion and standard deviation) were chosen to maximize the likelihood of the observed frequencies and are therefore called the best fit parameters. The program also calculated the χ^2 statistic for goodness of fit. In the χ^2 goodness of fit test the null hypothesis being tested was that the observed data came from the selected distribution with the given parameter estimates. If, under this hypothesis, the probability P of obtaining a value for χ^2 greater than that calculated was >0.05 then the hypothesis could not be rejected at the 5% level. That is, the selected distribution with the given parameter values provided one possible model for the data.

Errors

(1) There is a slight operator error in drawing around the image which is usually below 3% at the magnification used.

(2) The most significant error results from large cells having larger nucleoli than small cells. The magnitude of this error was measured by serial reconstruction (see below).

(3) A further error may result from the assumption that nucleolus-containing 1.5 μm sections pass through the middle of a spherical cell. Since the nucleolus is not absolutely central, nor the cell spherical, some error must result, but it is felt that this error is probably unbiased, that is, different cell types and different ages probably suffered the same magnitude of error.

SERIAL RECONSTRUCTION

Serial 1.5 μm sections from one ganglion from a 54-day-old mouse were mounted on a glass slide and stained with methylene blue. Two areas of the ganglion at depths of 100 μm and 400 μm into the ganglion were examined, each using about 15 consecutive sections. For each section outlines of cells, nuclei, nucleoli, and capillaries were made on an acetate sheet at a magnification of x 1500 using a x 100 oil immersion Reichert objective and a drawing tube attachment. The individual acetate sheets were palced in order between perspex sheets and any neuron with a complete nucleus in the series was numbered. Using this method it was possible to ascertain: (1) the number of nucleoli per cell, and their size; and (2) the number of sections of each cell which would have been included in the area measurements, using the same subjective criteria for judging which nucleolar sections were acceptable.

Photomicrographs (x 5100) were taken with a Zeiss photomicroscope and Reichert x 100 objective at the level of maximum diameter for each nucleolus, and cross-sectional area measurements were made of the cell, nucleus and nucleolus. Where more than one nucleolus existed, the maximum measured area for both nucleus and cell was used.

Results

The results to be described comprise: (1) counts of the numbers of neurons in mouse L_3 DRG; (2) frequency distribution histograms of cell areas measured using Epon sections; (3) mathematical analysis of these histograms into component populations; (4) the relationship of nuclear size to cell body size in Epon sections; and (5) an estimate of the bias in the frequency distribution histograms of area measurements due to nucleolar size.

CELL COUNTS

The numbers of neurons counted in 10 μm paraffin sections of L_3 ganglia at various postnatal ages are shown in Table 1 and plotted in Fig. 1A. The straight line regression shown was calculated using a Sumlock Compucorp statistical calculator. This is not significantly different from zero at the 5% level, showing no correlation between cell number and mouse age. The apparent downward trend in cell number with age is therefore not significant at this level. The range of cell numbers uncorrected for multiple nucleoli in the adult (50–70 days) was 5326–6233 per L_3 ganglion. In Fig. 1B the percentage of counted cells with two or more nucleoli in the same section (Table 1) is plotted against age. Again this regression line is not significantly different from zero at the 5% level, showing no correlation between this

Table 1. The counts of total numbers of neurons in L_3 DRGs. These were found by counting all neurons with nucleoli visible in every alternate 10 μm section throughout the ganglion. These numbers were then doubled to find the total number. The percentages of those cells counted which had more than one nucleolus visible in the nucleus are recorded in the last column. Data from this table is plotted in Fig. 1.

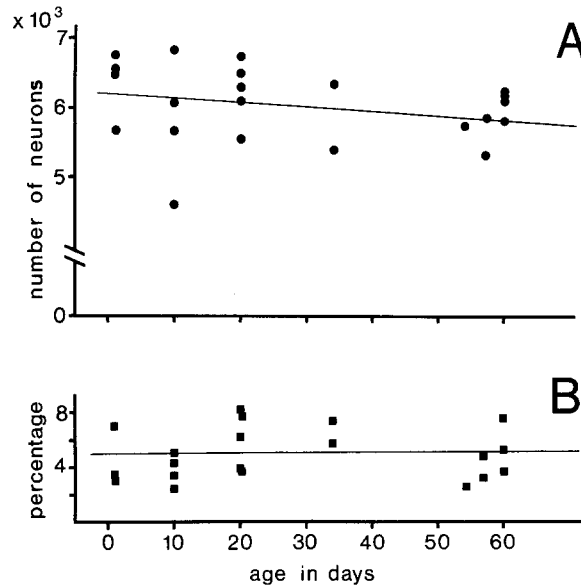| Mouse No.	Age (days)	Number of cells per L_3 ganglion		Mean number/mouse	Percentage of cells with > 1 nucleolus
1	1	5676		5676	3.03
2	1	6530		6530	7.07
3	1	6742	7468	7195	3.48
4	10	7298	6362	6830	2.45
5	10	5802	6334	6068	4.38
6	10	5692		5692	3.37
7	10	4588		4588	5.1
8	20	6030	6948	6489	3.83
9	20	5450	6690	6070	3.77
10	20	5544		5544	8.3
11	20	5764	6782	6273	6.27
12	20	6746		6746	7.86
13	34	6344		6344	7.4
14	34	5388		5388	5.72
15	54	5756		5756	2.61
16	57	5326		5326	3.37
17	57	5876		5876	4.98
18	60	5818		5818	not counted
19	60	6134		6134	3.75
20	60	6140		6140	5.37
21	60	6233		6233	7.68

Fig. 1.(A) The number of neurons per L_3 ganglion (ordinate) is plotted against the postnatal age of the mouse in days (abscissa). Each point is from one animal, that is, when two ganglia from the same animal were counted their mean is plotted. The correlation coefficient for the linear regression line is $r = -0.203$, $n = 21$. **(B)** The percentage of the neurons counted in A which had more than one nucleolus (ordinate) is plotted against postnatal age in days on the abscissa. Again the linear regression line is plotted: $r = 0.062$, $n = 20$.

percentage and mouse age. The data in Fig. 1B indicates that approximately 5% of the cells counted had more than one nucleolus and the counts are therefore subject to a slight overestimate, the magnitude of which depends on how many nuclei are split between two sections with at least one nucleolus in each. We do not have sufficient data to estimate the size of the error but these values are used for comparative purposes and the error appears to be the same at all ages.

ANALYSIS OF FREQUENCY DISTRIBUTION HISTOGRAMS

Frequency distribution histograms of neuronal cross-sectional areas are shown in Figs. 2, 3 and 5. They appear to have more than one component distribution. They were analysed by two methods.

First method
Using this method solutions were found using three normally distributed populations, but not using two (Fig. 2). This figure is included to illustrate the difficulties inherent in the interpretation of this type of data since the maximum likelihood program provided possible solutions using two normal distributions only (see below), and it has to be assumed that this is the most likely solution.
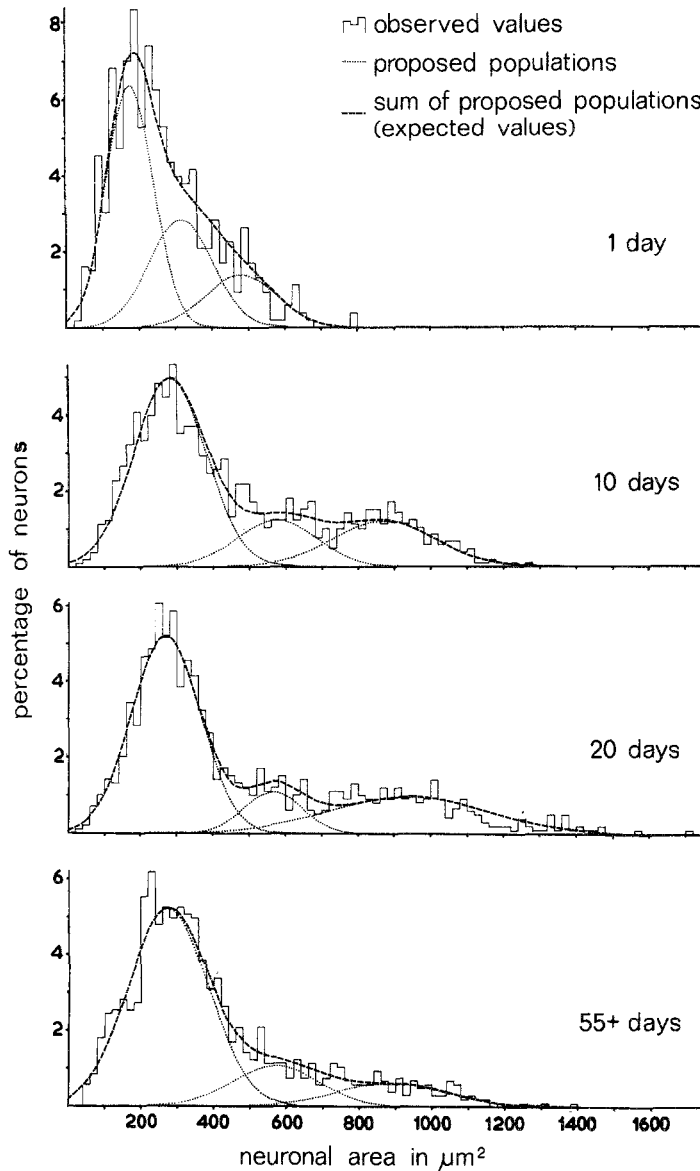
Fig. 2. First method of analysis of frequency distributions. The summed frequency distribution histograms (observed values) for cross-sectional areas of neurons in several L_3 ganglia for each of the ages plotted. The dotted lines show the proposed values for the component normal distributions. These are derived from that set of parameters (means, proportions and standard deviations) supplied by the user which together resulted in the best fit (lowest value of χ^2). These component distributions were added to find the expected values shown by the dashed line. In each case the χ^2 test between expected and observed gave a probability of >0.05, showing that the postulated results were not significantly different from the observed at the 5% level and these parameter values therefore provided a possible solution to the histogram. No solutions involving only one or two normal distributions could be found by this method.

Second method, using the Maximum Likelihood Program

In all 17 ganglia, best fit solutions (dashed lines, Fig. 3) were found with only two component normal distributions for which the χ^2 statistic showed no significant difference between the expected (dashed lines) and the observed at the 5% level. Examples of the frequency distribution histograms and their solutions using the best fit parameters given by the MLP program are shown in Fig. 3. In Fig. 3A—D, results from individual ganglia are shown. In E—H, all the data from ganglia for a particular range of ages was added. A clearly defined peak of one distribution comprised of the smaller cell is seen for each ganglion with a much more widespread distribution of larger cells. Although the size ranges overlap considerably, size is the only measure of the cells available at this stage in the analysis, and the two distributions will therefore be called small-cell and large-cell populations respectively. The best fit parameters for each ganglion, and their means for each age are set out in Table 2. The mean sizes for the large-cell populations (Table 2, column 3) and the small-cell populations (Table 2, column 6) were plotted in Fig. 4A to show how these varied with postnatal age. The small-cell population mean increased between 1 and 10 days but by 10 days had reached a plateau. The mean of the large-cell population, on the other hand, increased greatly between 1 and 20 days, but at some time after 20 days it decreased in size. Since there is no change with increasing age of either cell number (see Fig. 1A) or of the proportion of cells in the large-cell population (Fig. 4B), it seems that the average cell size actually decreased, that is, presumably individual cells of the large-cell population increase and subsequently decrease in size. The proportion of cells in the large-cell population as measured using this technique was variable (see Table 2, column 5, and Fig. 4B). Some of this is probably sampling error due to the odd shape of the ganglion and the infrequency of the sections counted (at only 120 μm intervals) and the fact that, in this material, large cells tend to be grouped together and to be nearer the surface of the ganglion. For this reason any ganglia with incomplete connective tissue capsules around them were discarded from this count. The regression line in Fig. 4B was not significantly different from zero at the 5% level. That is, no correlation could be demonstrated between the proportion of large cells in L_3 and the postnatal age of the mouse.

Fig. 3. Second method of analysis of frequency distribution histograms. (A-D) Examples of frequency distribution histograms of cell areas for single ganglia at each of the ages shown. (F—H) Summed frequency distribution histograms of cell cross-sectional areas from all the ganglia measured at each of the ages shown. In each case n is the number of cell areas measured. Superimposed are the normal distributions (calculated populations) of the small- and large-cell populations calculated from the best fit parameters provided by the MLP program (for the data see the ganglia marked with asterisks in Table 2). Also superimposed is the summed frequency distributions of the small- and large-cell populations (expected values). In all cases χ^2 test between the expected values and the observed showed a probability of >0.05. That is, there is no significant difference at the 5% level and the calculated values are therefore a possible solution to the histograms in each case. For each histogram, n is the number of neurons measured from that ganglion.
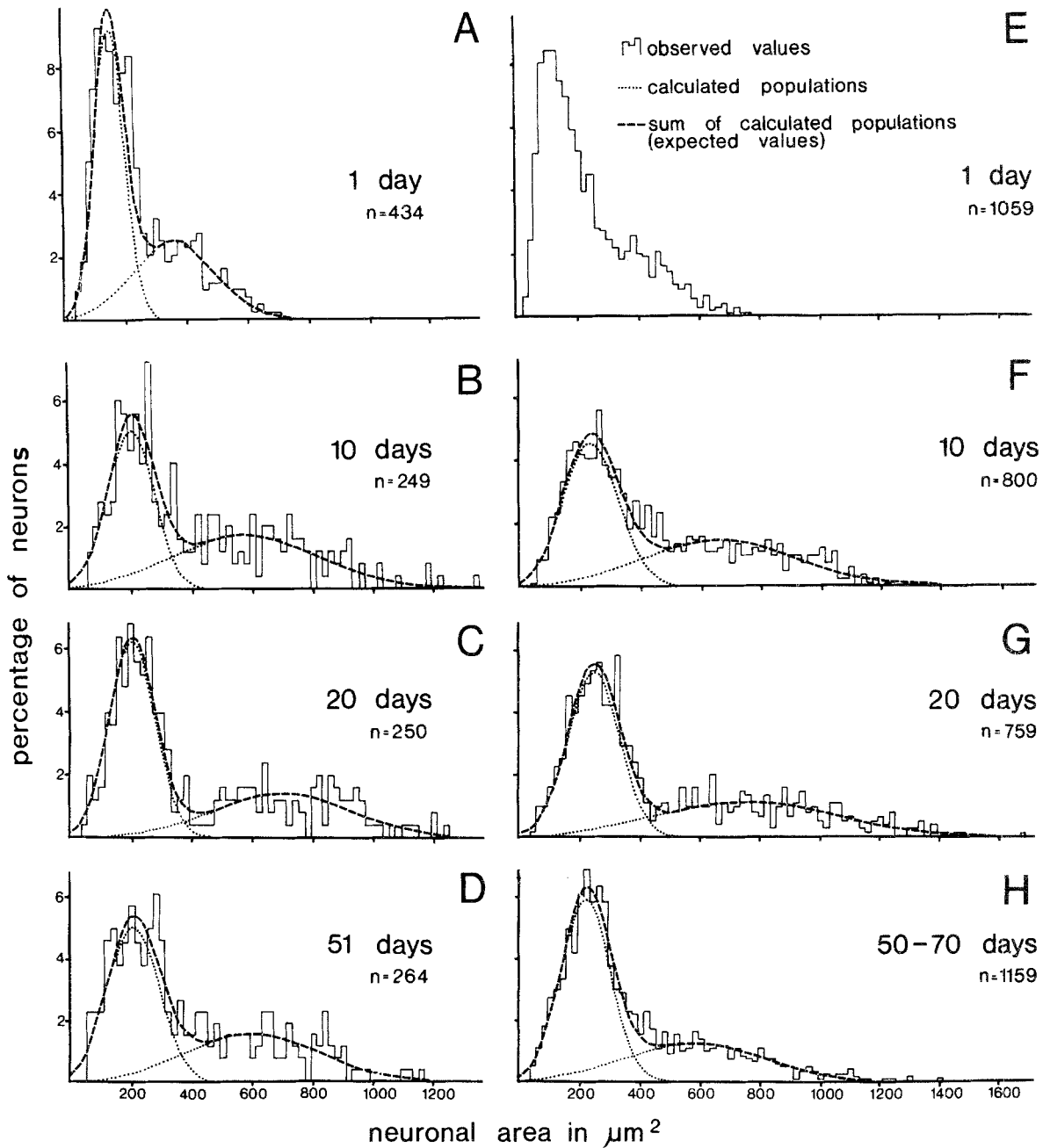
The one day ganglion in A was sampled at 60 μm intervals through the ganglion. All measurements on the other 16 ganglia were on sections taken at 120 μm intervals. In E no solution was found because the means of the two populations for individual ganglia differ widely (see Table 2, columns 3 and 6), possibly due to greater difficulty of fixation in very young animals and/or a natural variation in maturity of the ganglia immediately postnatal.

Table 2. Cell population parameters derived from the MLP program. This table gives the best fit parameters (columns 3—7) provided by the MLP program for the frequency distribution histogram of cell area from each ganglion measured. In all the ganglia, cells were measured in sections at 120 μm intervals with the exception of the one day ganglion with 434 measurements, which was sampled every 60 μm. Column 3 is the mean cross-sectional area for the large-cell population in μm. Column 4 is the standard deviation about that mean. Column 5 gives the percentage of the total number of cells counted which were included in the large-cell population. This is uncorrected for the bias caused by larger cells having larger nucleoli (see Results). Column 6 gives the mean cross-sectional area for cells of the small-cell population, and column 7 gives the standard deviation about that mean. Column 8 gives the values of χ^2 between the expected (that is, the distribution generated by the best fit parameters in columns 3—7) and the observed distribution. In all cases the probability is >0.05 which means that for each ganglion the parameters shown provide a possible solution to the frequency distribution histogram of cell cross-sectional areas obtained.

In each of the columns 3, 5 and 6 the mean value of the parameters and their standard deviation (S.D.) is given for each age group of ganglia delimited by the solid horizontal lines.

| Column No. 1	2	Population 1 Large cells			Population 2 Small cells		8	9	10
		3	4	5	6	7			
Age (days)	No. neurons measured	Mean	S.D.	%	Mean	S.D.	χ^2	d.f.	P
1	392	443	143.1	44.0	199	69.3	35.3	24	0.1—0.05
1*	434	369.8	135.9	42.1	185.5	50.7	18.7	20	0.7—0.5
1	269	284.3	105.6	32.4	131.8	39.4	4.55	12	0.95—0.98
2	288	301.3	120.4	37.7	140.5	45.9	10.25	14	0.8—0.7
Mean	349	349		39.1	157.5				
S.D.		± 72.3		± 5.2	± 29.8				
10	314	788	220.3	36.0	270	100.2	39.9	27	0.1—0.05
10*	249	596.5	242	52.0	219.6	76	22.5	24	0.7—0.5
10	239	687	255.1	46.1	278.1	111.3	34.0	28	0.3—0.2
Mean		690.5		44.7	255.7				
S.D.		± 95.8		± 8.1	± 32.0				
20	282	845.8	299	42	271.7	83.5	12.9	27	0.99—0.98
20*	250	716	227	40.4	220	76	17.41	23	0.8—0.7
20	229	724	380	44.7	287	90.3	34.1	23	0.1—0.05
Mean		761.7		42.3	259.3				
S.D.		± 72.3		± 2.1	± 35				
34	229	605	233	48.0	207	67	8.37	21	> 0.99
34	249	746	248	39.4	251	90	23.7	25	0.7—0.5
Mean		675.5		43.7	229				
S.D.		± 99.7							
51*	264	606	223.1	44.5	221	87.4	19.4	25	0.8—0.7
52	214	590.5	308.5	47.0	242.4	70.2	20.7	19	0.5—0.3
54	265	543.3	196.5	27.5	235.4	74.4	26.5	17	0.1—0.05
54	195	492.9	218.8	35.9	234.5	86.1	14.6	17	0.7—0.5
72	224	633	260	47.0	241.1	92	42.5	29	0.1—0.05
Mean		558.2		40.4	234.9				
S.D.		± 51.0		± 8.5	± 8.5				
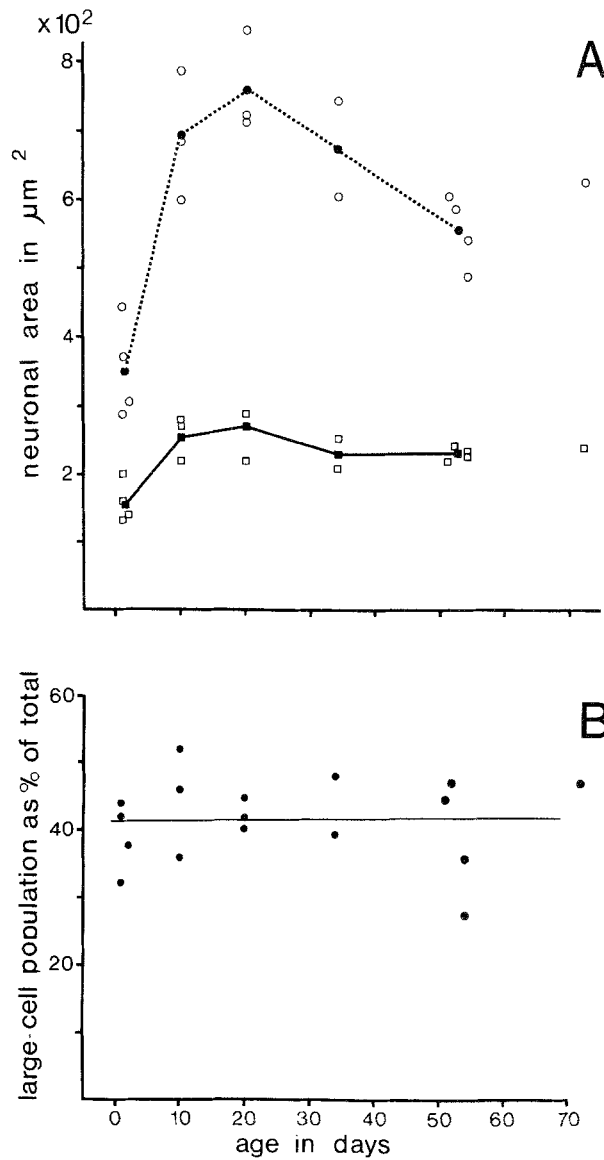
Fig. 4.(A) The mean neuronal cross-sectional areas (ordinate) for the small-cell population (squares) and the large-cell population (circles) from the MLP solutions to the frequency distribution histograms are plotted against postnatal age in days. For the data see Table 2. Results from individual mice are plotted with open symbols. The filled symbols show the means of groups of results at 1–2 days, 10, 20, 34 and 51–54 days. (B) For each ganglion the large-cell population as a percentage of the total number of cells measured on the ordinate is plotted against postnatal age (abscissa). This percentage is derived from the best fit parameter given by the MLP program (see Table 2, column 5). It is uncorrected and therefore an over-estimate of the real percentage of large neurons (see Results). The linear regression line is plotted (r = 0.012) and is not significantly different from zero at the 5% level.

Large light and small dark cells

Using the above methods, cells from two ganglia were measured and, at the same time, each cell was sorted according to the staining properties of the cytoplasm with methylene blue into either (a) light – lightly stained, with a patchy or clumped looking cytoplasm, or (b) dark – evenly and more deeply stained. For examples of such light and dark cells see Fig. 6. All cells were sorted although a decision was extremely difficult to make for a few cells (for example, 4/149 in the 51 day ganglion). The MLP best fit solution for both 1 and 51 day ganglia again involved two normal distributions, whereas for each age, populations of only dark cells or only light cells could be fitted by one normal distribution alone (see Fig. 5). The MLP
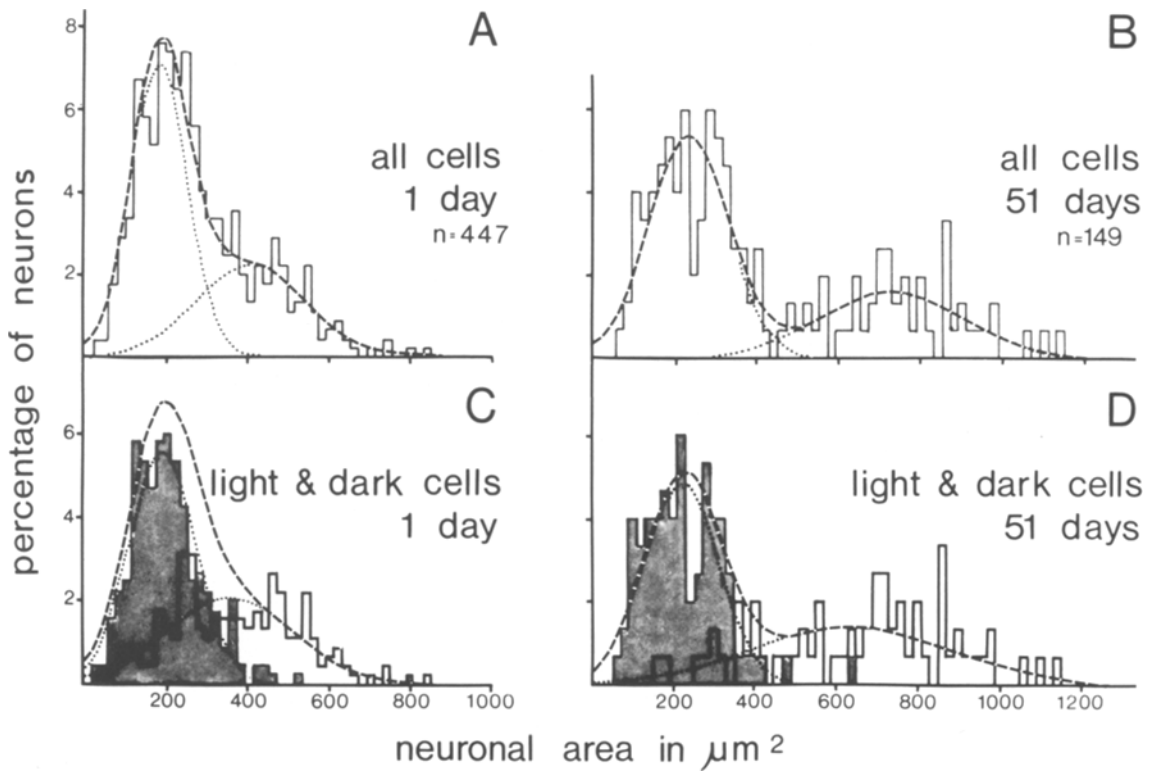

Fig. 5. The data and statistics for this figure are given in Table 3. (A and B) Frequency distribution histograms of cell areas for a one day and a 54 day ganglion respectively, analysed in precisely the same way as described for Fig. 3. No significant difference exists between the dashed line (expected) and the histogram (observed) at the 5% level. (C and D) The frequency distribution histograms of all dark cells (stippled) and all light cells (unshaded) from the overall distributions seen in A and B. Using the MLP program a single normal distribution could fit each of the light or dark cell curves such that χ^2 between observed and expected was >0.05. These distributions are shown by a dotted line in each case. The summed light and dark cell distributions are shown by the dashed line.

best fit parameters for these populations are shown in Table 3. The means for the large-cell and light cell populations for both ages were fairly close considering the difficulty of finding very accurately the means of such a flat spread out distribution when partially overlapped by another distribution. The parameters of the small-cell and dark cell populations in both cases were very close. It therefore seems reasonable to assume that the small-cell and large-cell populations as found using the MLP program are not distinguishable from the dark and light cell populations described subjectively by so many workers.

Table 3. The MLP best fit parameters for the histograms shown in Fig. 5 are listed. Lines 1 and 4 give the large-cell and small-cell population best fit parameters for the overall distributions shown in Fig. 5A and B, lines 2 and 5 give best fit parameters (single normal distributions) for the light cells only from these ganglia, lines 3 and 6 are similar for dark cells. %: In lines 2 and 5 the number of cells subjectively assessed as light is given as a percentage of the total number measured in that ganglion. No: gives the number of cells measured for each histogram. Statistics: χ^2, degrees of freedom (d.f.) and probability (P) between each histogram (observed) and its associated best fit solution (expected).

	Cell		Large- or light cell population			Small- or dark cell population		Statistics			See
Day	Type	No.	Mean	S.D.	%	Mean	S.D.	χ^2	d.f.	P	Fig. 5
	(1) All	447	419	134	37	197	71	19.3	23	>0.6	A
1	(2) Light	185	374	157	41	—	—	26	22	>0.2	C
	(3) Dark	262	—	—	—	208	85	17.7	13	>0.1	C
	(4) All	149	749	172	35	244	98	9.8	16	>0.8	B
51	(5) Light	65	665	246	43.6	—	—	7.3	9	>0.6	D
	(6) Dark	84	—	—	—	230	93	6.8	9	>0.6	D

SERIAL RECONSTRUCTION

The complete nuclei of 41 cells were serially reconstructed. Photomicrographs of each cell at the level of the nucleolus from the serial reconstruction could be sorted into only two cell types: 22 cells stained lightly with a patchy appearing cytoplasm (Fig. 6A–D), and 18 cells stained more deeply and evenly (Fig. 6B, C and D). One cell out of 41 was not classifiable in this manner. The two groups of cells will be called light and dark neurons. More than one nucleolus was seen in 10/22 light cells and in 9/18 dark cells, however, usually only one of these was large. In only 5/41 cells were there two nucleoli of similar size.

The serial reconstructions made it possible to count the number of sections

through each cell which would have been included in the cell area frequency distribution histograms described above. The same subjective criteria for selection on the basis of nucleolar sections was used (see Methods: Cell area measurements). It was found that because nucleoli are considerably larger in the larger cells, more sections of a large cell than of a small cell would have been included in the counts. When this number of sections was plotted against the cell size, it was found that, on average, at the mean areas for the large-cell and small-cell populations, the large cells would have been measured in three sections and the small cells in two. This is a direct estimate of the bias involved in the measurement of proportions of cells in the two populations, and it seems therefore that the large-cell population would have been overestimated by a factor of approximately 3/2 in this 54 day ganglion.

The mean percentage of cells in the large-cell population of the adult (50—70 day) mouse was found to be about 40%. Using the above factor to correct the percentage of large cells and taking into account the consequent reduction of the total by $\frac{1}{3}$ x 40% as follows:

$$\frac{2}{3} \times 40 \times \frac{100}{100 - \frac{1}{3} \times 40} \% = 30.77\%$$

the corrected percentage of cells in the large-cell population is about 30%, and 70% of the cells would therefore be included in the small-cell population. The magnitude of this error is probably very similar for the three ages since numbers of cells, proportions in each population and percentage with >1 nucleolus do not vary significantly with age.

Relationship of cell size to nuclear size
Fig. 6E shows the relationship of nuclear to cell cross-sectional area at the level of the largest nucleolar section in the 41 cells measured from the photomicrographs. It is perhaps more useful to think in terms of the surface areas of the nucleus and cell since the surface area of a sphere is 4 x the cross-sectional area measured through the centre of that sphere. One small cell was not classifiable as either light or dark. It had scant cytoplasm that was evenly stained to a shade intermediate between the light and dark cells. It is indicated on the graph by a filled triangle. The graph shows that cell area varies more with nuclear area for light than for dark cells. A regression line A drawn through all the cells shows a high degree of correlation between the two parameters throughout the entire population. Regression lines L through only the light cells and D through the dark cells plus the unidentified cell are also shown. The coefficients of correlation show a greater degree of correlation between nuclear and cell cross-sectional area for light than for dark cells. In order to test whether the two regression lines together, one through the dark cells (D) and one through the light cells (L) (model 1), provided a significantly better fit than the regression line
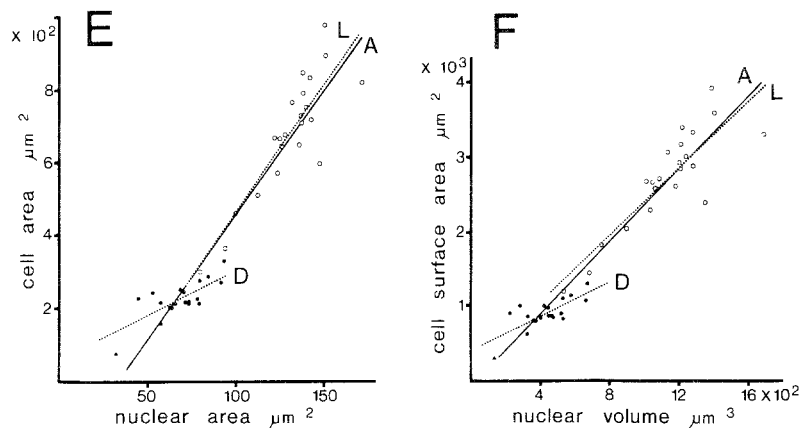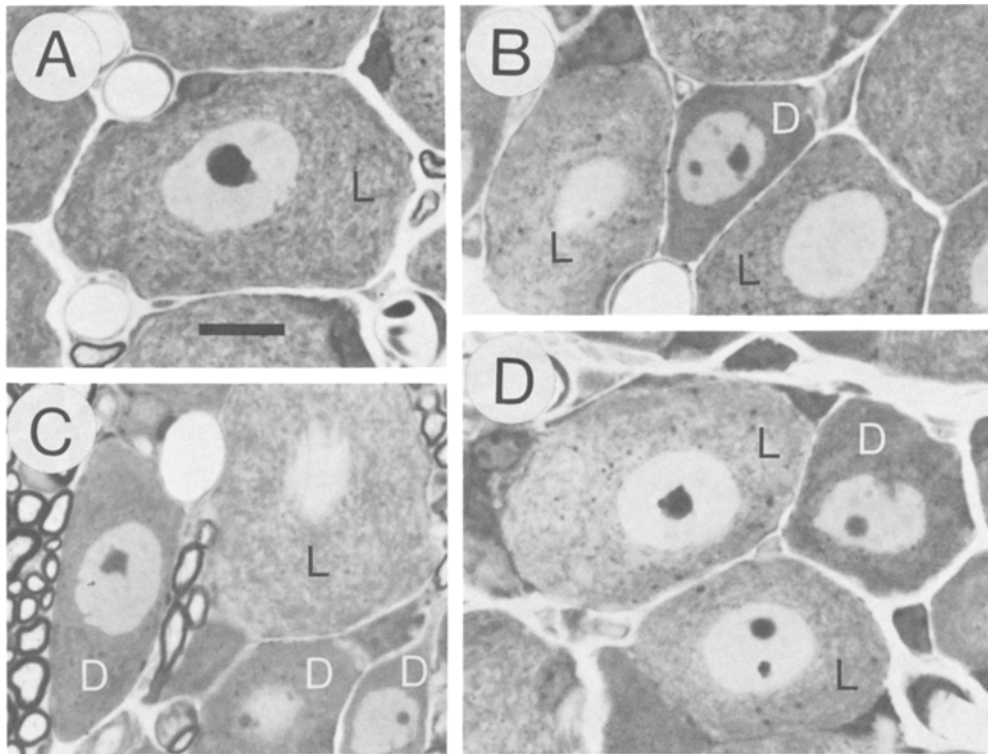
Fig. 6.(A–D) Photomicrographs of methylene blue stained 1.5 μm sections of L_3 DRG neurons from a 54-day-old mouse from the serial reconstruction series. Photographs were taken at the level of the largest nucleolar section of the central cells in A (light) and B (dark), of the dark cell to the left in C, and the upper light cell in D. Cells classified (see text) as light and dark are designated with an L or D respectively. Calibration bar in A = 10 μm and applies to all figures. **(E and F)**. The data in these graphs (see Table 3) are derived from cell measurements made at the level of the largest nucleolar section in the serial reconstruction series. Regression lines A include all cells, regression lines L include only those with light cytoplasm (open circles) and regression lines D included cells with dark cytoplasm (filled circles) plus the unidentified cell shown as a filled triangle.

(Graph E) Regression lines: (A) $r = 0.951$, $n = 41$; (L) $r = 0.87$, $n = 22$; (D) $r = 0.763$, $n = 19$.

(Graph F) Regression lines: (A) $r = 0.927$, $n = 41$; (L) $r = 0.859$, $n = 22$; (D) $r = 0.768$, $n = 19$. In both graphs E and F, the two regression lines L and D together provide a statistically better fit than regression line A (see text).

(A) through all the cells (model 2) the following test was applied:

ΣS is the sum of squares of differences between individual points and the regression line and d.f. is the degrees of freedom.

Model	Residuals	Degrees of freedom
1 A (all)	ΣS_A	$n_D + n_L - 2 = 39$
2 $\{$ D (dark)	ΣS_D	$n_D - 2 = 17$
L (light)	ΣS_L	$n_L - 2 = 20$
$\Rightarrow$ for model 2	$\Sigma S_D + S_L$	$n_D + n_L - 4 = 37$
$\Rightarrow$ difference between model 1 & 2	Diff $\Sigma S = \Sigma S_A - (\Sigma S_D + \Sigma S_L)$	$(n_D + n_L - 4) - (n_D + n_L + 2)$ $= 2$

$$F_{2,37} = \frac{\Sigma S_A - (\Sigma S_D + \Sigma S_L)}{37} - \frac{\Sigma S_D + \Sigma S_L}{2}$$

$F_{2,37} = 11.52$. Using F tables the probability P was found to be < 0.01.

This test shows that a significantly better fit for the data is provided by two regression lines D and L than by the single regression line A. This is also true if the filled triangle is included in the light cell population. However, it is possible that a continuous non-linear relationship may exist depending not on cell type but on size alone. Further attempts to find a good straight line fit involving all the cell types, using the slope of a log/log plot of the above data led to Fig. 6F in which nuclear volume is plotted against cell surface area (calculated from the cross-sectional areas, and assuming a spherical cell with no processes). Although this graph was the nearest to a straight line obtained, still the light and dark cells appear to have differing slopes on the graph. Three regression lines were again plotted: A, all cells; L, light-cells; and D, dark cells. Again a statistically better fit at the 1% level was provided by the two regression lines L and D than by one regression line only (A). ($F_{2,37} = P < 0.01$). This was true whether the filled triangle cell was included in the light or the dark cell population.

This shows therefore, that the light cells differ from the dark cells in the relationship of their nuclear volume or surface area to the total cell surface area, if it is assumed that the cell body is spherical and that the cell processes are not included in the calculation.

Discussion

This paper describes a method of analysis of frequency distributions of cell size into their component populations assuming normal distributions of the parameters measured. This assumption is based not only on precedent (Harding, 1949; Hughes, 1973) and on the commonly held view that many biological phenomena tend to

normal distribution through random biological variations about a mean, but also on the knowledge that the procedures involved are likely to add further random errors at each stage, thus increasing the likelihood of each population being well described as a normal distribution. Random errors added at each stage should not affect the mean of the populations (except in the case of shrinkage due to fixation), but rather should increase the standard deviation of the observations about the population mean.

Using the MLP program, solutions could be found in all ganglia for two normal distributions but never for one, although solutions were found involving three populations by a cumbersome manual method. The two population solution is more acceptable since it is the simpler solution and since any distribution can be more accurately fitted by a larger number of component distributions. By this token the reason that solutions could not be found by 'hand' for two distributions no doubt results from the much tighter constraints involved in a fit with the smaller number of distributions and therefore the greater number of iterations required to fulfil those constraints; iterations that can only be carried out conveniently by a computer.

It is difficult to reconcile these results with those of Kawamura and Dyck (1978) who suggest that three cell types are distinguishable by size on the basis of three peaks in their frequency distribution histogram of cell diameter in human L_5 DRGs. One possible explanation is that the wider spread of cell size in the human (up to $100\,\mu m$ diameter) than in the mouse (up to $45\,\mu m$ diameter) leads to improved resolution of cell types by size alone. However, even taking into account the different measurements made, the distributions shown in their histograms differ so greatly from the present data that a more fundamental difference between human L_5 and mouse L_3 ganglia must be considered.

Certainly the present data and its statistical analysis suggests that in the mouse L_3 DRG, neurons fall into two distinct normally distributed populations, the large-cell and the small-cell populations. It was also found that these populations have somewhat differing developmental characteristics since the large cells increase in size between birth and 20 days after which time their size decreases, whereas the small cells increase in size before 10 days after which time their size remains constant. The reason for this difference is not known. Donaldson and Nagasaka (1918) found that the ten largest ganglion cells (in one section only per ganglion) increased in size throughout the life of the rat. This may be associated with the fact that rats continue to grow throughout life. In the mouse, however, this continued growth of DRG cells does not apparently occur in either cell type even if only the very largest cells are considered (see Fig. 3).

From the present evidence it appears that the large-cell population consists of cells which can be classified as light staining, and similarly that the small-cell population consists of dark cells. Since large light cells have such a wide distribution there is considerable overlap between the two populations and the use of an arbitrary cut-off point to distinguish between the two cell types can therefore be very mis-

leading. For this reason it would seem to be more useful if future subjective distinctions between cell types were made, whenever possible, on the basis of light or clumped appearance, and dark or evenly stained appearance.

A further difference between the large light and small dark cells is the relationship of cell size to nuclear size. In large light cells these parameters are closely related whereas in small cells a wide range of nuclear sizes is associated with a very small range of cell sizes. No explanation for this difference can be offered at present. It is possible, however, that nuclear size and total cytoplasmic volume or cell surface area are related in a similar manner in the two cell types and the difference seen between the cell types is due to differing geometry outside the perikaryon, which was not taken into account in these measurements. The length and thus the volume of nerve cell processes may vary enormously not only in the periphery but also depending on where they terminate in the spinal cord or higher centres, and this therefore has to remain an unknown quantity at present.

The number of cells in the mouse L_3 ganglion appears remarkably constant with age. This agrees with data on rat ganglia (Hatai, 1902) but is in contrast with the counts of Duchen and Scaravilli (1977) who found much lower cell numbers in mouse DRGs at birth than they found subsequently. In the human, Emery and Singhal (1973) showed no significant change in the numbers of cells in thoracic ganglia from birth to over 70 years of age, although cell loss in human DRGs has been described by Gardner (1940) and Scharf and Blumenthal (1967), particularly after the age of 35.

The serial reconstruction showed that large cells were measured about 1.5 times more frequently than the small cells due to their larger nucleoli. Using this value the corrected percentage of large cells in 50—70 day ganglia was 31%, whereas the uncorrected percentage was 40%.

There has been some speculation in the past as to the possible interchange of cells between one type and another (Hatai, 1902). Tewari and Bourne (1962) show evidence that within the small- and large-cell groups the cells undergo continuous metabolic cycles and suggest that the small cells themselves may be a stage in the total cell cycle of the ganglion. In the mouse there is no evidence for this, since from birth to 70 days the total number of neurons is virtually constant and the proportion of cells in each population is apparently unchanged. The most important evidence against any such transformation is provided by tritiated thymidine autoradiography (Lawson and Biscoe, 1979) which shows that the neuroblasts which stop dividing first in the foetus become the larger neurons in the adult, cells with later cell birthdays become the small neurons. The size distribution of the cells which form early has a wide scatter and is very reminiscent of the shape of the distribution of large light cells in this paper. Such a relationship between cell type and time of formation of neurons would not be apparent if much interchange of cells between the cell types were to occur.

If these neurons are to be classified further than the two major classes described here, a functional allied with a quantitative anatomical approach is probably

necessary. On the basis of phase contrast and electron microscopy further subdivisions of the two major cell types have been suggested by Andres (1961) and by Duce and Keen (1977), the latter on the basis of the staining properties of the Golgi body. Such subdivisions may reflect either permanent types of cells possibly associated with their sensory modality or transmitter types, or more transient properties such as changing rates of synthesis perhaps relating to neuronal activity and transmitter release. In this context it has already been demonstrated by Hökfelt *et al.* (1976) that both Substance P and somatostatin are to be found in detectable quantities in small DRG cells but apparently never in the same cell. The relative sizes of the two cell types are not reported. However, this evidence would indicate two functional divisions of the small dark cell population.

In conclusion, then, evidence is presented for the existence in the dorsal root ganglion of two major non-interchangeable neuronal types with different developmental properties, size and appearance. Further subdivisions have been described in the literature but functional studies need to be allied with a quantitative approach in order to distinguish relatively permanent differences in cell properties from the superimposition of transient metabolic states.

References

ABERCROMBIE, M. (1946) Estimation of nuclear population from microtome section. *Anatomical Record* 94, 239–47.

ANDRES, K. H. (1961) Untersuchungen über den Feinbau von Spinalganglien. *Zeitschrift für Zellforschung und mikroskopische Anatomie* 55, 1–48.

BISCOE, T. J., LAWSON, S. N., MAKEPEACE, A. P. W. and STIRLING, C. A. (1978) Apparatus for the measurement of micrographs and other experimental records. *Journal of Physiology (London)* 277, 5–6P.

BOUTRY, J. M. and NOVIKOFF, A. B. (1975) Cytochemical studies on Golgi apparatus, GERL and lysosomes in neurons of dorsal root ganglia in mice. *Proceedings of the National Academy of Sciences (U.S.A.)* 72, 508–12.

CAMMERMEYER, J. (1967) Artifactual displacement of neuronal nucleoli in paraffin sections. *Journal für Hirnforschung* 9, 209–24.

DONALDSON, H. H. and NAGASAKA, G. (1918). On the increase in the diameter of nerve cell bodies and of the fibres arising from them during the later phases of growth (albino rat). *Journal of Comparative Neurology* 29, 529–52.

DUCE, I. R. and KEEN, P. (1977) An ultrastructural classification of the neuronal cell bodies of the rat dorsal root ganglion using zinc iodide-osmium impregnation. *Cell and Tissue Research* 185, 263–77.

DUCHEN, L. W. and SCARAVILLI, F. (1977) Quantitative and electron microscopic studies of sensory ganglion cells of the Sprawling mutant mouse. *Journal of Neurocytology* 6, 465—81.

EMERY, J. L. and SINGHAL, R. (1973) Changes associated with growth in the cells of the dorsal root ganglion in children. *Developmental Medicine and Child Neurology* 15, 460—7.

GARDNER, E. (1940) Decrease in human neurones with age. *Anatomical Record* 77, 529—36.

HATAI, S. (1902) Number and size of the spinal ganglion cells and dorsal root fibres in the white rat at different ages. *Journal of Comparative Neurology* 12, 107—24.

HARDING, J. P. (1949) The use of probability paper for the graphical analysis of polymodal frequency distributions. *Journal of the Marine Biological Association of the United Kingdom* 28, 140—53.

HÖKFELT, T., ELDE, R., JOHANSSON, O., LUFT, R., NILSSON, G. and ARIMURA, A. (1976) Immunohistochemical evidence for separate populations of somatostatin-containing and substance-P containing primary afferent neurones in the rat. *Neuroscience* 1, 131—6.

HUGHES, A. (1973) The development of dorsal root ganglia and ventral horns in the opposum — A quantitative study. *Journal of Embryology and experimental Morphology* 30, 359—76.

KALINA, A. and WOLMAN, M. (1970) Correlative histochemical and morphological study in the maturation of sensory ganglion cells in the rat. *Histochemie* 22, 100—8.

KAWAMURA, Y. and DYCK, P. J. (1978) Evidence for three populations by size in L5 spinal ganglion in man. *Journal of Neuropathology and Experimental Neurology* 37, 269—72.

LAWSON, S. N. and BISCOE, T. J. B. (1979) Development of mouse dorsal root ganglia: an autoradiographic and quantitative study. *Journal of Neurocytology* 8, 265—74.

LAWSON, S. N., CADDY, K. W. T. and BISCOE, T. J. B. (1974) Development of rat dorsal root ganglion neurones. Studies of cell birthdays and changes in mean cell diameter. *Cell and Tissue Research* 153, 399—413.

LAWSON, S. N., MAY, M. K. and WILLIAMS, T. H. (1977) Prenatal neurogenesis in the septal region of the rat. *Brain Research* 129, 147—51.

LIEBERMAN, A. R. (1976) Sensory ganglia. In *The Peripheral Nerve* (edited by LANDON, D. N.) pp. 188—278. London: Chapman and Hall.

OHTA, M., OFFORD, K. and DYCK, P. J. (1974) Morphometric evaluation of the first sacral ganglia of man. *Journal of the Neurological Sciences* 22, 73—82.

PALAY, S. L. and CHAN-PALAY, V. (1974) *Cerebellar Cortex, Cytology and Organisation.* pp. 322—336. Berlin, Heidelberg, New York: Springer-Verlag.

PARFIANOWICZ, J., HAWRYLKO, S., PIETRZAK, J. and KMIEC, B. (1971) Morphology and cytochemistry of the nerve cells of the spinal ganglia. *Folia Morphologica (Warszawa)* (English Translation) 30, 423—31.

PRETO PARVIS, V. (1954) Distribution of two types of nerve cells with different evolutional characteristics in the spinal ganglia of the cat. *Monitore zoologico italiano (Firenze)* 63, 352—4.

SARRAT, R. (1970) Zür Chemodifferenzierung des Ruckenmarks und der Spinalganglien der Ratte. *Histochemie* 24, 202—13.

SCHARF, J.-H. and BLUMENTHAL, H.-J. (1967) Neuere Aspecte zur altersabhängigen Involution des Sensiblen Peripheren Nervensystems. *Zeitschrift für Zellforschung und mikroscopische Anatomie* 78, 280—302.

SCOTT, S. G. (1912) On successive double staining for histological purposes. *Journal of Pathology and Bacteriology* 16, 390—8.

TEWARI, H. B. and BOURNE, G. H. (1962) Histochemical evidence of metabolic cycles in spinal ganglion cells of rat. *Journal of Histochemistry and Cytochemistry* 10, 42—64.

YAMADORI, T. (1971) A light and electron microscopic study on the post-natal development of spinal ganglia. *Acta anatomica nipponica (Tokyo)* 45, 191—205.